Fermilab FERMILAB-Conf-00/259-E CDF October 2000

CDF/ANAL/MIN_BIAS/CDFR/5415

-

Soft and Hard Interactions in $p\bar{p}$ Collisions at $\sqrt{s}$ = 1800 and 630 GeV

F. Rimondi[a] for the CDF Collaboration

[a]Dipartimento di Fisica,Istituto Nazionale di Fisica Nucleare, Sezione di Bologna,
viale Berti Pichat 6/2, 40127 Bologna, Italy

Proton-antiproton events collected with the CDF minimum-bias trigger at $\sqrt(s)$ = 1800 and 630 GeV are studied splitting the full event sample in a *soft* subsample of events with no energy clusters above 1.1 GeV and in the subsample of the remaining events. Detailed and precise analyses of the multiplicity and transverse momentum distributions as well as of the correlation of the average p_t and of its dispersion with the multiplicity are performed for the two samples. Comparisons of the results and of their dependence from the center of mass energy show clear differences in their behaviours. The results support important and unexpected scaling properties of the *soft* sample.

1. INTRODUCTION

Hadron interactions are commonly classified in hard and soft interactions. However highly pure samples of events generated by hard parton interactions can only be collected selecting the rare events with clear high E_t cluster identification. High cross-section events collected with minimum bias trigger are to be thought as a mixture of a large number of soft interactions with a component of hard interactions events. The fraction of these latter events decreases with the jet transverse energy of the event and globally increases with the c.m.s. energy. The properties of events coming from minimum bias trigger could be the result of the different production mechanisms which generate different kind of events. Their energy dependence partially reflects the enrichment in hard interactions due to the rise of the hard parton interaction cross-section with increasing energy. In this analysis a splitting procedure of the full minimum bias sample in two subsamples, one highly enriched in soft interactions and the other enriched in hard interactions, is applied. The two subsamples are then analysed comparatively at two different c.m.s. energy, $\sqrt{s}$ = 1800 and 630 GeV. The results evidence some interesting unobserved properties of the *soft* interaction sample and a remarkable, mainly unpredicted, scaling behaviour between 630 and 1800 GeV.

2. DATA SET AND EVENT SELECTION

The experiment has been performed with the CDF detector at the Fermilab Tevatron Collider. The CDF apparatus has been described elsewhere [1]; here only the parts of the setup utilized for the present analysis are discussed.

Data were collected with a minimum bias trigger during Run 1A, 1B, 1C (1800 GeV) and 1C (630 GeV). This trigger requires coincident hits in the beam-beam counters (BBC), located at 5.8 m from the nominal vertex position and covering 5.4 units in η, in coincidence with a machine-crossing signal. For the present measure the charged tracks detected in the Central Tracking Chamber (CTC) have been used. The CTC is a drift chamber covering a η interval of about three units with full efficiency for $|\eta| \leq 1$ and $p_t \geq 0.4$ GeV/c. The tranverse energy flux was measured in the full calorimeter system, globally covering from -4.1 to 4.1 in η.

In the offline selection:

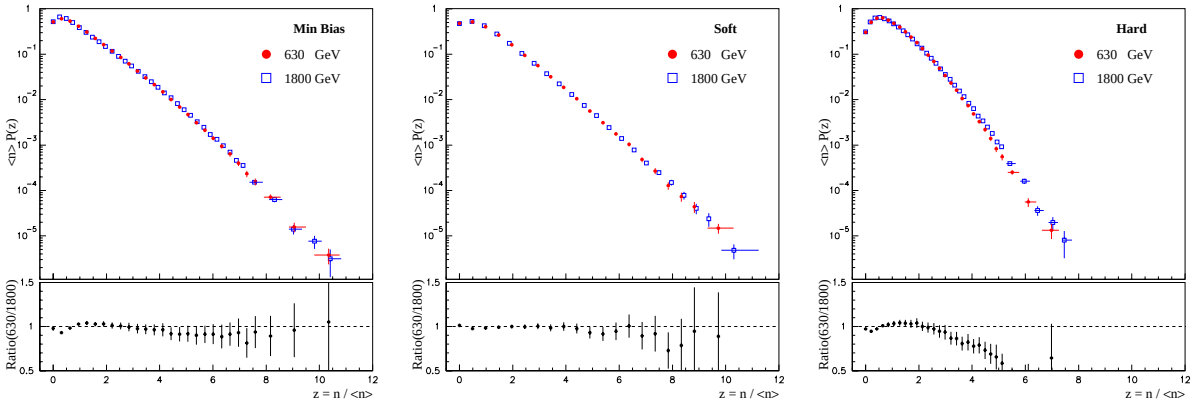

Figure 1. Multiplicity distributions for the full MB, the *soft* and the *hard* samples at 1800 and 630 GeV; data are plotted in KNO variables. On the bottom of each plot, the ratio of the two distributions at the two energies is shown.

- all events were required to pass a cosmic ray filter based on the time-of-flight measurement performed by the scintillator counters of the central calorimeter;
- runs having an exeedingly high number of events with more than 250 calorimeter towers hit were excluded;
- to avoid multievent energy superposition in the calorimeters, events with a second primary vertex were rejected;
- vertex Z cut: $|Z_{vert}| \leq 60$ cm is required;
- events with CTC multiplicity greater than zero but no towers hit in the central calorimeter were rejected;
- events with one or more tracks of $p_t > 50$ GeV/c were rejected.

Out of about 3,300,000 events at $\sqrt{s}$=1800 GeV (run 1A+1B+1C), 2,321,962 pass the above cuts. At $\sqrt{s}$=630 GeV (run 1C) 2,036,994 remain after the cuts out of about 2,600,000 triggers.

3. TRACK SELECTION

The following cuts were applied to tracks beside the standard quality cuts required by the CTC reconstruction program:

- tracks with impact parameter (distance between the track extrapolation and the z axis) $d_0 > 0.5$ cm were rejected;
- tracks with z matching $|Z_0 - Z_v| > 5$ cm were rejected.

In order to ensure full CTC efficiency only tracks with $p_t \geq 0.4$ GeV/c and $|\eta| \leq 1.0$ were accepted.

All the data presented here have been corrected for track finding and reconstruction inefficiency as well as for the physical background contamination coming from γ conversion, particle decays and secondary interactions.

Given the above cuts the charged track multiplicity, throughout our analysis, is defined by the number of selected CTC tracks in each event. The mean p_t of the event, when not differently stated, is defined as:

$$\bar{p}_t = \frac{1}{N} \sum_i^N p_{t_i} \qquad (1)$$

where N is the number of tracks of the event.

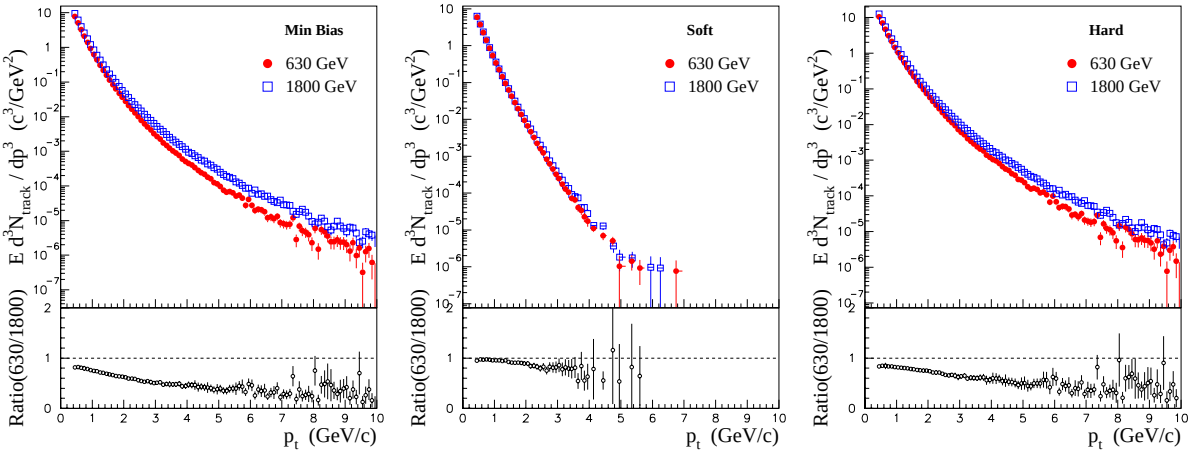

Figure 2. Transverse momentum distributions for the full MB, the *soft* and the *hard* samples at 1800 and 630 GeV. On the bottom of each plot, the ratio of the two distributions at the two energies is shown.

4. SELECTION OF *SOFT* AND *HARD* INTERACTIONS

The recognition of jet structures is almost unambiguous when large E_t jets are present, but it is really difficult to identify and separate jets with E_t lower than 5 GeV or below [2]. So the identification of soft, semi-hard and hard interactions below that transverse energy is largely a matter of definition. In this analysis we define *soft* interaction any event in which no cluster of a minimum tranverse energy of 1.1 GeV is observed in $|\eta| \leq 4.1$. Clusters of towers in the Central and End-Plug Calorimeters were reconstructed via the jet-finding cone algorithm with radius $R = (\Delta\eta^2 + \Delta\phi^2)^{1/2} = 0.7$. With the above selection a cluster may consist of a seed tower of $E_T > 1$ GeV and an adjacent tower of at least 0.1 GeV. Calorimeter cluster finding has been checked and corrected for energy loss in the calorimeter cracks, in the regions $|\eta| < 0.02$ and $1.1 < |\eta| < 1.2$, with a track cluster algorithm. A track cluster has been defined as one track of $p_t > 0.7$ GeV/c with at least a second track in a cone $R = (\Delta\eta^2 + \Delta\phi^2)^{1/2} = 0.7$ and with a $p_t \geq 0.4$ GeV/c.

The total Min-Bias sample was splitted into two subsamples:

- events with no clusters (from now on *soft* sample)
- events with at least 1 cluster (from now on *hard* sample)

Since it is not possible to avoid any ambiguity in the identification of very low energy clusters, our selection of *soft/hard* events is essentially a definition. The dependence of all the results from the threshold E_T energy has been tested by repeating the analysis at a cluster energy threshold of 3 GeV. The different threshold choice strongly influences the inclusive distributions, as it has to be expected, but does not change substantially the characteristic different behaviour of the *soft/hard* samples. In particular it preserves the scaling behaviour of the *soft* distributions and correlations at the two energies.

5. DATA ANALYSIS

5.1. Inclusive Distributions

Some inclusive distributions, namely multiplicity and transverse momentum distributions, are

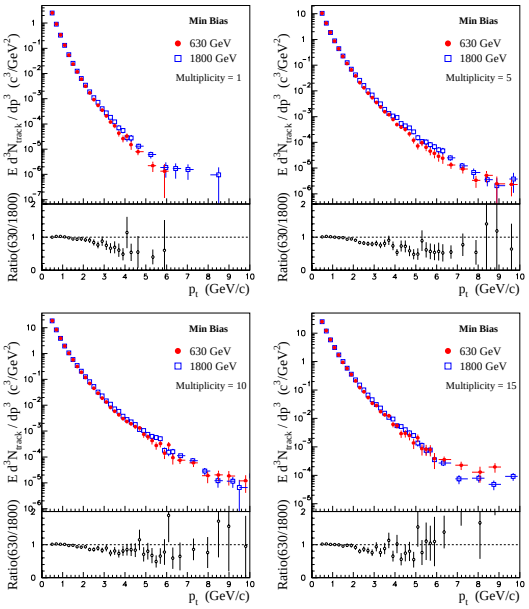

Figure 3. Transverse momentum distributions at fixed multiplicity (multiplicity = 1, 5, 10, 15) for the full MB samples at 1800 and 630 GeV. At the bottom of each plot the ratio of the two above distributions is shown.

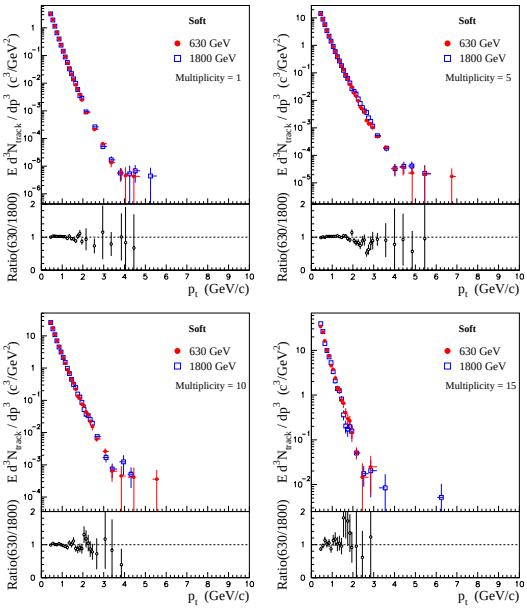

Figure 4. Same as Fig. 3 for the *soft* samples.

examined first.

Fig. 1 shows the multiplicity distributions for the full MB samples at 1800 and 630 GeV. Data are plotted in KNO variables. The comparison of the distributions at the two energies shows a weak violation of the KNO scaling as it is expected in a limited phase space region [3]. In the same figure the same comparison is made for the *soft* and *hard* samples separately. The ratios of the overstanding distributions are plotted in the bottom part of each plot in Figs. 1. The behaviour of the *soft* and *hard* samples is different and in particular a remarkable superposition of the distributions at the two energies is observed for the *soft* sample, suggesting that the KNO scaling violation in the full sample comes from the *hard* component.

Transverse momentum distributions are shown in Fig. 2 for the full MB sample, the *soft* and *hard* sample respectively.

As for the multiplicity distributions, the ratios of the distributions at the two energies are shown in the bottom of each plot in this figure. The steeper slope of the *soft* distributions is expected as it merely reflects the absence of events with high p_t jets. Completely unexpected instead is the suggested invariance with the c.m.s. energy of the p_t distributions at fixed multiplicity in the *soft* sample. This can be seen in Fig. 4 where in each plot the p_t distributions at fixed multiplicity, 1, 5, 10 and 15 respectively, are shown for 1800 and 630 GeV superimposed. The same distributions for the same values of multiplicity are plotted in Figs. 3 and 5 for the full MB and for the *hard* samples respectively.

The independence from the c.m.s. energy of the p_t distribution at fixed multiplicity will appear much clearly in the correlation of the average p_t as a function of the multiplicity (see next subsection).

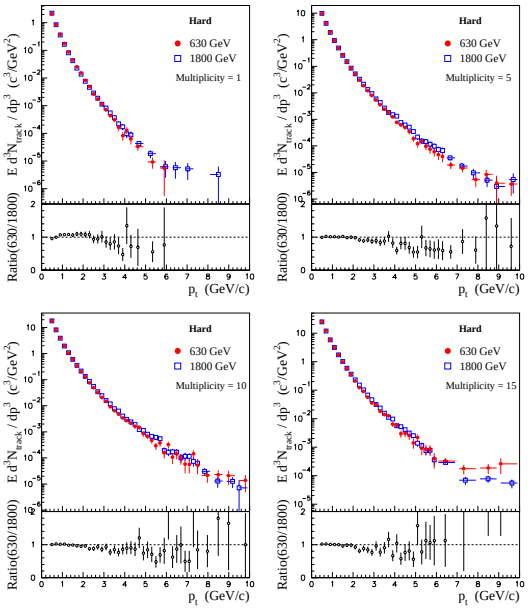

Figure 5. Same as Fig. 3 for the *hard* samples.

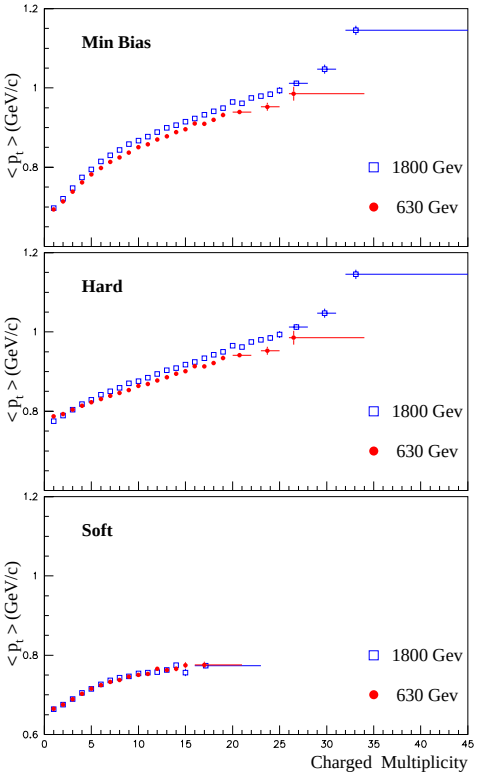

Figure 6. Mean transverse momentum vs multiplicity at 1800 and 630 GeV. Here the $\langle p_t \rangle$ is computed as the sum of the p_t of all the measured trackss at the given multiplicities divided by their number (see Eq.(1) of the text).

5.2. Dependence of Mean Track p_t on Charged Multiplicity

The correlation between mean p_t and charged multiplicity is known since its first observation by UA1 [4] and successively investigated at the ISR [5] and at the Tevatron Collider energies [6], but its theoretical explanation is still not completely known. Among the proposed interpretations is that the increase is due to the contribution of high E_t interactions (*minijets*), but quantitative previsions are really poor when compared with experimental results [7]. Actually we measure the average p_t in two ways. In the first, the mean p_t is obtained by Eq. (1) above. It is simply the sum of the p_t of all the measured charged tracks divided by their number. Results from this method are summarized in Fig. 6.

In the second way the p_t distribution at fixed multiplicity is fitted to the form:

$$f(p_t) = A \left(\frac{p_0}{p_t + p_0} \right)^n \qquad (2)$$

and the average p_t is computed from the fitted function. This second determination gives a value of the mean p_t pretty close to the true mean p_t, while in the first case it is simply the mean p_t of the observed tracks. The results of the present measure of the dependence of the mean p_t on the multiplicity as obtained by the fit are shown in Fig. 7 for the full minimum bias, the *soft* and the *hard* samples at the two analysed energies.

Here is to be noted the good superposition of the plots at the two energies for the *soft* sample. This invariance of the average p_t dependence from the multiplicity with the c.m.s. energy confirms the previous result of the invariance of the p_t dis-

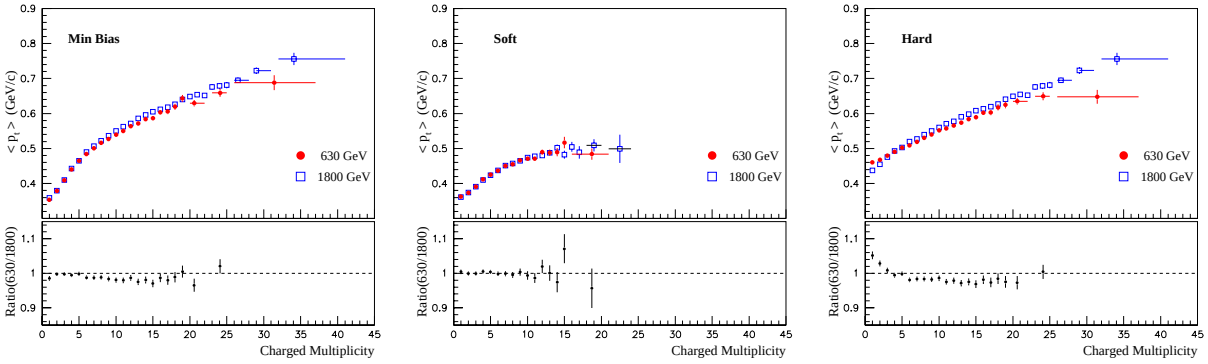

Figure 7. Mean transverse momentum vs multiplicity for the full MB the *soft* and the *hard* samples at 1800 and 630 GeV. Here the $\langle p_t \rangle$ is obtained by fitting the p_t distributions at each multiplicity to the form (2). On the bottom of each plot, the ratio of the two curves at the two energies is shown.

tributions at fixed multiplicity with $\sqrt{s}$. Still to be noted in Figs. 7 is the clear difference of the correlation in the *soft* and *hard* samples.

5.3. $\langle \mathbf{p_t} \rangle_{\mathbf{ev}}$ Dispersion versus Multiplicity

Event-by-event fluctuations on the mean p_t have been shown to be a valid tool to investigate the collective behaviour of soft multibody production. In slightly different ways this tool has been applied to analyze experimental data [8–10]. Following the approach of [8], the dispersion of the mean event p_t is defined for each multiplicity by:

$$D_m\left(\bar{p}_t\right) = \frac{\langle \bar{p}_t^2 \rangle_m - \langle \bar{p}_t \rangle_m^2}{\langle p_t \rangle_{sample}} \qquad (3)$$

Brackets $\langle\rangle$ indicate average over all events with a given multiplicity m, while $\bar{p}_t$ is here the mean p_t of Eq.(1).

The dispersion D is expected to decrease with increasing multiplicity and to converge to zero when $m \to \infty$ if only pure statistical fluctuactions are present. Conversely, an extrapolation to a non-zero value would indicate the presence of non statistical fluctuations from event to event in the $\langle p_t \rangle_{ev}$. This indeed is what was found in [8] and, in different ways, in [9,10]. Large non poissonian event-by-event fluctuations of the mean event p_t are a consequence of the particle correlations in the multibody final state [11]. In Fig. 8 the result of the present measure of the dispersion from Eq. (3) as a function of the inverse multiplicity for the full minimum bias sample is shown

The points deviate from linearity at high multiplicity, particularly at $\sqrt{s} = 1800$ GeV. The separate analysis of the dispersion versus multiplicity for the *soft* and *hard* samples, shown in the same figure, confirms that this effect is related to the contribution of the jet production which, as discussed in [12], increases the event-by-event fluctuations.

Comparing our *soft* sample results with [8], where the hard jet production has a much lower cross section than at our energies, it has to be noted that our points drop at high multiplicity (multiplicity $\gtrsim 10$), which was not observed in [8]. Moreover this effect cannot lead to the conclusion of an extrapolation different from zero at infinite multiplicity. Finally, the dispersion as a function of the inverse multiplicity for the *soft* samples has an almost constant ratio at the two energies, which is not true for the *hard* samples.

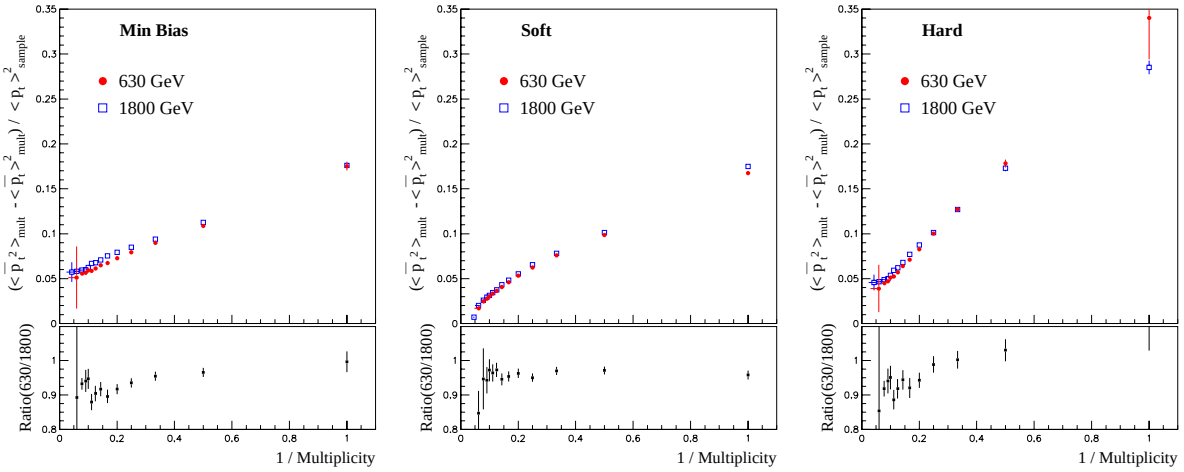

Figure 8. Dispersion of the mean event p_t as a function of the inverse multiplicity for the full MB, the *soft* and the *hard* samples at 1800 and 630 GeV. At the bottom of each plot, the ratio of the two curves at the two energies is shown.

6. CONCLUSIONS

Assuming that hard parton interactions in $\bar{p}p$ scattering, whatever is the Q^2 between the interacting partons, eventually develop into observable particles clusterized in jet cones in the final state, and pushing the cluster identification to the lowest energy threshold, we separate minimum bias events in *soft* and *hard* interaction enriched samples. Comparing the behaviours of the two samples and of the samples at the two energies, we obtain the following results.

- The multiplicity and tranverse momentum inclusive distributions of *soft* and *hard* interactions are significantly different, the differences being similar at both energies. The multiplicity distributions of *soft* interactions follow the KNO scaling going from $\sqrt{s}$ = 630 to 1800 GeV. This is not true for the *hard* interactions. Concerning *soft* interactions, the p_t distributions at fixed multiplicity scale with energy. That is to say, independently from the c.m.s. energy, the number of charged particles in the final state fix their momentum distribution. The p_t distributions integrated over all the multiplicities at the two energies differ only by the weight given by the different multiplicity distributions.

- The dependence of the mean p_t on multiplicity, already measured at 1800 GeV, definitely shows, with the high statistical precision of this measurement, a structure which is not reproduced by the current theoretical or phenomenological model. It is to be noted that a small rise of the mean p_t is still present in the *soft* sample where any hard parton interaction is at least strongly suppressed. The remarkably good scaling of the dependence for the *soft* samples confirms the result quoted above (a).

- The dependence of the dispersion of the $\langle p_t \rangle_{ev}$ on the inverse multiplicity shows a non linear behaviour which was not previously observed. Furthermore the comparison of the *soft* to the *hard* sample indicates that the weak rise at multiplicity greater than $\sim$10 is essentially due to the presence of hard parton interactions.

In the same multiplicity region the slope of the dispersion in the *soft* sample allows to exclude a non-zero extrapolation at infinite multiplicity. The ratio of the *soft* samples at the two energies is flat as a function of multiplicity, that is not true for the *hard* samples.

In all the distributions and correlations studied the *soft* subsample is compatible with the hypothesis of scaling with the c.m.s. energy, which is a relevant and new result.
In this frame of *soft* interactions, the dynamical mechanism of multiparticle inelastic production appears to be invariant with c.m.s. energy at least in our energy interval. Therefore the properties of the observable final state are determined only by the number of (charged) particles, that is by the increased phase space.

REFERENCES

1. F. Abe *et al.*, Nucl. Instrum. Methods **A271** 387 (1988), and references therein.
2. F. Abe *et al.*, Phys. Rev. **D56** 3811 (1997); Phys. Rev. Lett. **79** 584 (1997); X.Wang, Phys. Rev. **D46** 1900 (1992); UA1 Collaboration, C.Albajar *et al*, Nucl. Phys. **B309** 405 (1988).
3. UA5 Collaboration, R.E. Ansorge *et al.*, Z.Phys. **C43** 357 (1989); K. Alpgard *et al.*, Phys. Lett. **B121** 209 (1983).
4. UA1 Collaboration, G. Arnison *et al.*, Phys. Lett. **B118** 173 (1982).
5. A.Breakstone *et al.*, Phys. Lett. **B132** 463 (1983); Phys. Lett. **B183** 227 (1987); Phys. Lett. **B132** 458 (1983).
6. E735 Collaboration, T.Alexopoulos *et al.*, Phys. Lett **B336** 599 (1994); Phys. Rev. Lett. **60** 1622 (1988); Nucl. Phys. Proc. Suppl. **B25** 40 (1992); Phys. Rev. **D48** 984 (1993); N.Moggi, Nucl. Phys. Proc. Suppl. **B71** 221 (1999).
7. C. Hwa and X. Wang, Phys. Rev. **D39** 187 (1989).
8. K. Braune *et al.*, Phys.Lett. **B123** 467 (1983).
9. H.Appelshäuser, Phys. Lett. **B459** 679 (1999).
10. M.L. Cherry *et al*, Acta Phys. Pol. **B29** 2129 (1998).
11. M. Gaździcki, Eur. Phys. J. **C6** 365 (1999) and references therein.
12. F. Liu, Eur. Phys. J. **C8** 649 (1999).